LBL-28598
Preprint

Lawrence Berkeley Laboratory
UNIVERSITY OF CALIFORNIA

Submitted to Neurosurgery

A Compartmental Flow Model for Assessing Hemodynamic Response of Intracranial Arteriovenous Malformations to Stereotactic Radiosurgery

E.H. Lo, J.I. Fabrikant, R.P. Levy,
M.H. Phillips, K.A. Frankel, and E.L. Alpen

February 1990

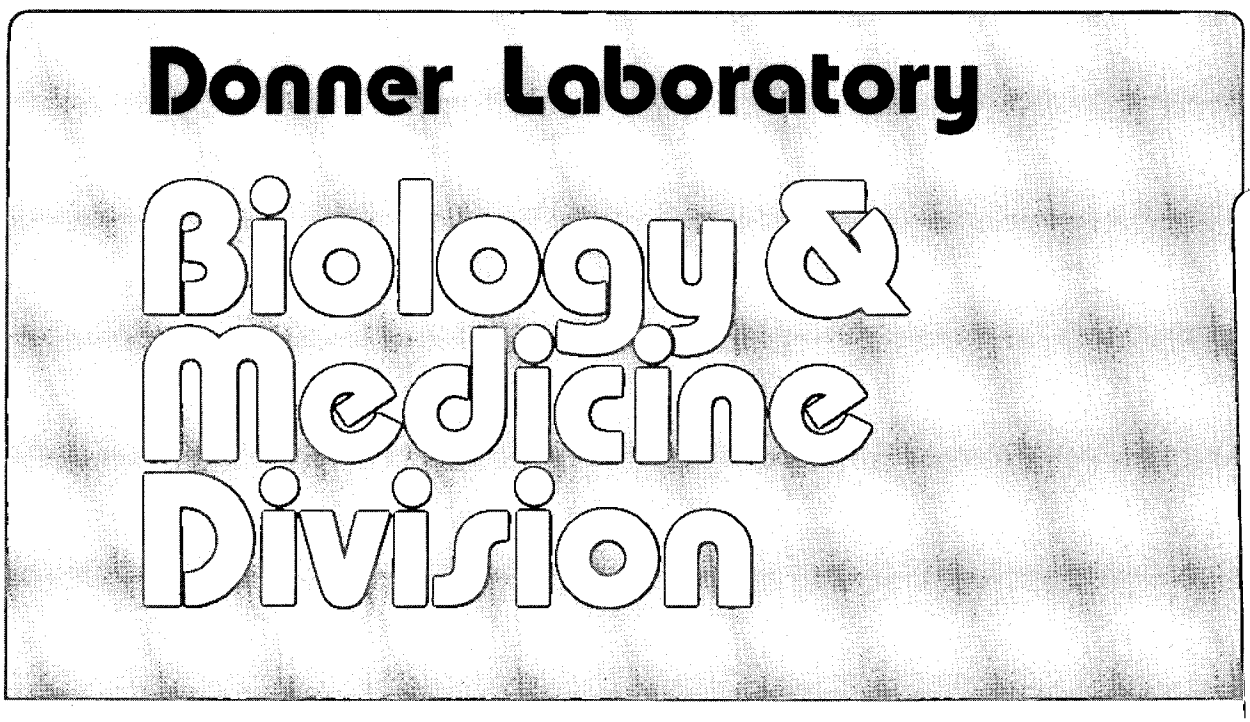

Prepared for the U.S. Department of Energy under Contract Number DE-AC03-76SF00098.

DISCLAIMER

A COMPARTMENTAL FLOW MODEL FOR ASSESSING HEMODYNAMIC RESPONSE OF INTRACRANIAL ARTERIOVENOUS MALFORMATIONS TO STEREOTACTIC RADIOSURGERY[1]

Eng H. Lo[1,2], Jacob I. Fabrikant[1,2,3], Richard P. Levy[1,2],
Mark H. Phillips[1], Kenneth A. Frankel[1], Edward L. Alpen[1,2]

[1] Donner Pavilion, Research Medicine and Radiation Biophysics,
Lawrence Berkeley Laboratory,
1 Cyclotron Road, Berkeley,
CA 94720

[2] Department of Biophysics and Medical Physics,
University of California, Berkeley

[3] Department of Radiology,
University of California, San Francisco

[1]Research supported by the Office of Energy, Health, and Environmental Research of the United States, Department of Energy under Contract DE-ACO3-76SF00098

ABSTRACT

Stereotactic radiosurgery has proven to be an effective method of treating deep and inaccessible or inoperable arteriovenous malformations (AVMs) of the brain. Complete radiation-induced obliteration of an angiographically-demonstrable AVM occurs after an average latent period of about 1-2 yr post-treatment. During this latent period, the probability of hemorrhaging remains prior to complete thrombotic obliteration, primarily because of hemodynamic alterations in and around the AVM as a result of the pathophysiological changes following radiation treatment. A hemodynamic compartmental flow model is proposed to describe this process and to analyze temporal alterations in blood flow rates and pressure gradients within the AVM. It is found that increases in pressure gradients across certain vascular structures within the AVM occur after treatment. However, the magnitude of these pressure alterations may be within the normal physiological variations in cerebrovascular blood pressure. It is also found that limiting radiosurgical treatment to only part of the entire arterial phase of the AVM volume may induce alterations in pressure gradients which persist in unirradiated vascular shunts, even after complete obliteration of the treated AVM volume. This may increase the probability of hemorrhage from the untreated shunts of the AVM. These pressure alterations induced by partial-volume radiosurgical treatment may also cause redistribution of regional cerebral blood flow (rCBF) resulting in increased flow through the untreated shunts of the AVM. Discussion includes the pathophysiological basis of the altered cerebral blood flow dynamics, and clinical examples of alterations leading to abnormal flow from persisting vascular shunts following stereotactic radiosurgery.

Key Words : arteriovenous malformation, cerebral hemodynamics, compartmental flow model, intracranial hemorrhage, regional cerebral blood flow, stereotactic radiosurgery

INTRODUCTION

The management of intracranial arteriovenous malformations (AVMs) is one of the most difficult areas of vascular neurosurgery. Stereotactic radiosurgery has proven to be an effective method of treating deep inoperable AVMs (1,4,5,7,8,9,13,14,15,16,19,20,22,28,29). Radiation injury to the AVM vessels causes endothelial cell damage and proliferation, intima degeneration, media degeneration and hyalin thickening, which leads to altered blood flow dynamics, hemostasis, and eventually thrombosis and obliteration of the AVM (1,7,10,16,28). Following radiosurgery, complete AVM obliteration may be observed to occur with an average latent interval of about 1-2 yr, depending on a number of factors, including AVM size, location, and treatment dose (4,5,8,9,15,16). Radiation-induced vascular and hemodynamic changes can be observed on cerebral angiography after an initial induction period of approximately 1 yr; irradiated vessels begin to narrow and blood flow dynamics are altered with conversion of high-volume, high-flow hemodynamics to a decreased flow rate and angiographic filling; complete closure of the AVM usually occurs after an additional year or more (7,8,9,15). The underlying pathophysiological mechanisms involved in this latency interval are not well understood, but are central to the clinical outcome of the treatment procedure. During this period when abnormal vascular shunts still remain patent and hemodynamic alterations occur, patients remain vulnerable to intracranial hemorrhage (15,16,28).

As the radiosurgically-treated AVM shunts narrow and close off, the distribution of pressure gradients and the regional cerebral blood flow (rCBF) patterns in the AVM, as well as in the surrounding cerebral vasculature, are expected to change considerably. It is not known whether the probability of intracranial hemorrhage increases during this period prior to closure because of progressive hemodynamic alterations. This information currently is based on clinical experience solely, but primarily in those patients who already have sustained one or multiple hemorrhages prior to treatment. An understanding of the temporal patterns of rCBF perturbations underlying this process would permit the introduction of

methods, where appropriate, that may influence treatment strategies.

A hemodynamic compartmental flow model of an angiographically-demonstrable AVM, based on anatomical structures described by Yamada et al (30,31), is proposed to simulate narrowing of blood vessels in the radiosurgically-treated AVM, and to simulate changes in blood flow rates and pressure gradients in different components of the AVM. The alterations following complete- and partial-volume treatments of AVMs are compared. For the purposes of this report, complete-volume treatment of an intracranial AVM means the inclusion of the entire arterial phase of the AVM (including all aberrant feeders and shunts) in the treatment target volume; any other cases where only portions of the entire arterial phase are targeted are considered to be partial-volume treatments. Potential clinical applications are presented as examples of hemodynamic alterations that may occur as a result of stereotactic radiosurgical treatment of AVMs.

METHODS

Compartmental Anatomy

The intracranial AVM model consists of three linked compartments : (1) arterial feeders that connect nearby arteries to the AVM, (2) thin shunting arterioles, and (3) central vessels of the AVM core which drain into the venous system (30,31) (Figure 1a, 1b). Each compartment may be considered to consist of a collection of parallel vessels of equal length with a Poisson distribution of vessel radii. Thus, each compartment can be defined by three variables: the length of the vessels l, the number of vessels N, and the mean radius of each distribution r. The subscripts F, S, C are used to denote the compartments of the feeding arteries, the shunting arterioles, and the core vessels, respectively.

Flow Dynamics

Laminar flow of a homogenous fluid along a tube can be described with Poiseiulle's equation (11,26):

$$Flow\ \ rate = \frac{\pi r^4 \Delta P}{8\eta l} \tag{1}$$

where

ΔP = pressure gradient across the tube

r = radius of the tube

η = coefficient of viscosity of the fluid

l = length of the tube.

Equation (1) serves as the biophysical basis for the AVM model. Flow rates through each compartment can be calculated as the total Poiseiullian flow through the collection of parallel tubes within each compartment. A constant Newtonian blood viscosity of 0.04 Poise is assumed. Equation (1) can be expressed as

$$flow\ \ rate = \frac{\Delta P}{R} \tag{2}$$

where hemodynamic resistance,

$$R = \frac{8\eta l}{\pi r^4} \tag{3}$$

For our model,

$$Flow_{AVM} = \frac{\Delta P_{AVM}}{R_{AVM}} \tag{4}$$

where the total hemodynamic resistance of the AVM is equal to the sum of the resistances in the feeding artery, shunting arteriole, and core vessel compartments, or $R_{AVM} = R_F + R_S + R_C$.

Hemodynamic resistances in the individual AVM compartments are

$$R_F = \frac{1}{\Sigma_f^{N_F} \frac{1}{Z_f}} \tag{5}$$

$$R_S = \frac{1}{\Sigma_s^{N_S} \frac{1}{Z_s}} \tag{6}$$

$$R_C = \frac{1}{\Sigma_c^{N_C} \frac{1}{Z_c}} \tag{7}$$

where N_F, N_S, N_C, are the total number of vessels in each compartment, and Z_f, Z_s, Z_c, are the individual resistances of the Poisson distribution of vessels in each compartment, so that

$$Z_f = \frac{8\eta l_F}{\pi r_f^4 P_{r_f} N_F} \tag{8}$$

$$Z_s = \frac{8\eta l_S}{\pi r_s^4 P_{r_s} N_S} \tag{9}$$

$$Z_c = \frac{8\eta l_C}{\pi r_c^4 P_{r_c} N_C} \tag{10}$$

For equations (8), (9), and (10), P_{r_f}, P_{r_s}, and P_{r_c} are the Poisson coefficients, so that $P_{r_f} N_F$, $P_{r_s} N_S$, and $P_{r_c} N_C$ represent the number of vessels in each compartment with a specific radius.

Pressure Gradients and Flow Rates

Table 1 lists the compartmental parameters selected to represent *small* (low-flow) and *large* (high-flow) intracranial AVMs. The relatively large number of vessels in parallel within each compartment results in a low hemodynamic resistance shunt. The hemodynamic resistance of each compartment is calculated using equations (5), (6), and (7), and the blood flow rate through the AVM obtained. There is only limited hemodynamic data available on AVMs because of the difficulty of performing intraoperative measurements. Batjer et al have demonstrated that hemodynamic alterations occur after flow-directed embolization of intracranial AVMs (2,3). Nornes and his colleagues (18,23,24,25) have used directional ultrasound and Doppler shift techniques to measure pressure gradients and blood flow rates in untreated AVMs prior to surgical resection; their measurements are used to adjust the initial parameters in our model. A pressure gradient of approximately 45 mmHg across the

AVM is assumed. Vessel sizes in each compartment are chosen based on representative AVM shunt sizes and structures discussed by Yamada et al (30,31): average radii of 1 cm for the feeding arteries; 0.1 cm for the shunting arterioles; 1 cm for the core vessels. The lengths of vessels in each compartment are assumed to be in the 1-5 cm range, which agrees well with average sizes of typical AVM vessels (23,30,31). Finally, the number of vessels in the three compartments are adjusted in order to reproduce the flow rates measured by Nornes et al (18,23,24,25) for *small* (low-flow, 150 ml/min) and *large* (high-flow, 440 ml/min) AVMs. Although actual vessel sizes and numbers will surely vary between individual AVMs, the values chosen are adequate for this initial analysis.

Application of the Model

The model may now be used to simulate the vascular and hemodynamic changes that occur after a variable initial induction period following radiosurgery. We have evaluated two different luminal narrowing rates. The first assumes a constant narrowing rate of 0.025 mm/mon. The second assumes that smaller vessels undergo narrowing more rapidly than larger vessels; therefore vessels with radii less than 0.2 mm would close off at a rate of 0.05 mm/mon and larger vessels at 0.025 mm/mon. These representative rates were chosen to produce AVM obliteration within periods comparable to those observed in radiosurgical clinical series (7,8,9,16).

The changing distribution of vessel radii in each compartment is followed over time, and the hemodynamic resistances and pressure gradients in each compartment are calculated. This permits the alterations in blood flow rate through the AVM to be determined. By changing the number of abnormal AVM vessels in each compartment that undergoes radiation-induced vessel narrowing, the compartmental flow model of the AVM is used to compare the consequences of complete- and partial-volume irradiation procedures. Two partial-volume irradiation examples are considered: (1) the entire volume of the central core compartment of the AVM is treated, but only partial volumes of the feeding arterial and shunting arteriole compartments are irradiated; (2) only partial volumes of all three

AVM compartments are irradiated. Selected clinical cases are presented as representative examples of hemodynamic alterations that may result from complete- and partial-volume stereotactic radiosurgery of large high-flow AVMs.

RESULTS

Complete-Volume Treatment

Blood flow rates are calculated for a *small* (low-flow, 150 ml/min) and a *large* (high-flow, 440 ml/min) AVM following complete-volume irradiation. Hemodynamic resistance and pressure gradients are demonstrated to be highest in the shunting arteriole compartment in both cases. Alterations in hemodynamic parameters following radiosurgery are calculated as radiation-induced luminal narrowing of AVM vessels occurs after a variable initial induction period (Figures 2 and 3): blood flow rates through the AVM are plotted versus time; blood pressure gradients in the three AVM compartments are plotted versus time.

Once radiation-induced hemodynamic changes begin, blood flow through the treated AVM decreases exponentially to zero and complete obliteration occurs within 6-12 mon for a *small* AVM (Figure 2a), and 10-14 mon for a *large* AVM (Figure 3a). Pressure gradients in the feeding arteries and the central shunts of the AVM core begin to fall immediately as flow decreases (Figures 2b, 2d, 3b, 3d). However, pressure gradients in the shunting arteriole compartment demonstrate an initial increase as AVM blood flow decreases (Figures 2c and 3c). This transient rise in pressure can be understood in terms of the strong dependence of hemodynamic resistance on the inverse fourth power of the vessel radius; vessels in the shunting arteriole compartment of the AVM are the smallest and therefore the relative change in radius in this compartment is the greatest. This causes the relative hemodynamic resistance of this compartment to rise as flow through the AVM decreases. This rise in pressure is eventually terminated when the vessels are obliterated completely and flow ceases. The pattern of changes in pressure gradients in all three AVM compartments are

demonstrated to be similar for *small* and *large* AVMs. However, pressure alterations persist for longer periods in *large* AVMs because they require more time for complete obliteration to occur.

Two different luminal narrowing rates were evaluated: (1) a radius-dependent rate where smaller vessels close off faster; (2) a radius-independent rate where all vessels close off at the same rate. It is demonstrated that there are no qualitative differences between these two different narrowing rates; the faster radius-dependent rate simply results in more rapid AVM obliteration. A radius-dependent luminal narrowing rate resulted in complete AVM obliteration in about 6 mon (Figure 2a) and 12 mon (Figure 3a) for *small* and *large* AVMs respectively; the slower radius-independent luminal narrowing rate resulted in complete AVM obliteration in about 12 mon (Figure 2a) and 16 mon (Figure 3a) for *small* and *large* AVMs respectively.

Case Report. A 38 year old white male with a large left temporal lobe AVM suffered a massive hemorrhage 4 mon prior to treatment. He was treated with stereotactic radiosurgery (27 GyE, 230 MeV/u helium ions); the radiation dose was delivered through 7 ports in 3 daily fractions to a target volume of 34,000 mm^3 covering the entire arterial phase of the AVM. Angiographic examination demonstrated complete obliteration of the AVM with restoration of normal cerebral blood flow patterns 1 yr after radiosurgery (Figure 4a-b).

Partial-Volume Treatment

When all abnormal vessels in the central core compartment are irradiated, but the feeding arterial and shunting arteriole compartments are irradiated incompletely (a situation that can occur in clinical situations), complete AVM obliteration may be achieved when all shunting vessels in the core compartment close off. However, obliteration of the AVM occurs after a much longer time (32-36 mon), and assumes a biphasic temporal pattern (Figure 5a). In the first phase, irradiated vessels in all three AVM compartments begin to close off, resulting in an initial decrease in total AVM blood flow. A plateau period follows as the larger vessels in the AVM core take a longer time to undergo luminal narrowing and

ultimate obliteration. The second phase of decrease in AVM blood flow begins when vessels in the central core compartment have narrowed sufficiently to cause an increase in the total hemodynamic resistance of the AVM. Eventually, all vessels in the core compartment are obliterated and blood flow through the AVM ceases. The pressure profiles demonstrate the expected exponential decrease in pressure in the feeding arterial compartment (Figure 5b), but there is an extended period of increased pressure gradient in the shunting arteriole compartment where pressure increases from about 36.5 mmHg to about 40 mmHg for approximately 15 mon (Figure 5c). A large increase in the pressure gradient also occurs transiently in the core vessel compartment; pressure increases from 1.5 mmHg to almost 45 mmHg in the 4-5 mon prior to complete AVM obliteration (Figure 5d).

When only 50% of all three AVM compartments are treated, it appears that total blood flow through the AVM does not reduce to zero. Blood flow through a *large* AVM decreases from a pre-treatment value of 440 ml/min to about 140 ml/min over a period of approximately 12 mon (Figure 6a). However, there are significant alterations in pressure gradients in the various AVM compartments; blood pressure in the feeding arterial and core compartments decrease (Figure 6b, 6d), but pressure in the shunting arteriole compartment increases from 36.5 mmHg to over 40 mmHg, and remains permanently elevated (Figure 6c).

Case Report. A 20 year old white male with a large right basal ganglia AVM suffered an intracranial hemorrhage 7 mon prior to treatment. Surgical clipping of selected vessels was performed to in an attempt to decrease AVM blood flow rate before radiosurgery. He was treated with stereotactic radiosurgery (20 GyE, 230 MeV/u helium ions); the radiation dose was delivered through 4 ports in 2 daily fractions to a target volume of 1,600 mm^3 covering only the anterior portion of the angiographically-demonstrable AVM volume (Figure 7a). Angiographic examination demonstrated obliteration of the targeted AVM volume with corresponding decrease in size of the anterior feeding vessels at 1 year after radiosurgery (Figure 7b). However, the posterior portion of the AVM remained patent, and

the feeding artery supplying this component of the AVM had increased in size, associated with an increased rate of blood flow through the persisting untreated AVM shunts.

DISCUSSION

The intracranial AVM is essentially an arteriovenous shunt that "short circuits" blood directly from the arterial system to the venous system. The absence of functional capillaries and the large number of pathological vessels in an AVM results in its low hemodynamic resistance and high blood flow rates. The high flow rates through these malformed vessels also increase their susceptibility to hemorrhage (17,27). It is presently unclear if hemodynamic alterations in and around a radiosurgically-treated AVM may increase the probability of hemorrhage prior to complete obliteration. A compartmental flow model, based on anatomical structures described by Yamada et al (30,31), is developed to analyze alterations in hemodynamic parameters of a radiosurgically-treated AVM.

Although the AVM is composed of tortuous clusters of abnormal shunts, and not a collection of straight vessels, the compartmental flow model appears to be an adequate method for modeling the functional hemodynamic characteristics of the AVM as it undergoes reaction to radiation injury and thrombosis. A convoluted tube with many turns and angles has been demonstrated to be equivalent, in terms of its hemodynamic resistance, to a straight tube of greater length (6). The linear sum of the typical vessel lengths in the three AVM compartments is not equal to the total AVM diameter. AVM vessels are usually tangled into a cluster and the actual size of the malformation is smaller than the linear sum of these hemodynamically equivalent straight vessel lengths.

All our calculations are based on Poiseiulle's equation for laminar flow; therefore all turbulent activity is precluded from the model. However, this does not appear to be a serious limitation since studies have shown that most AVM flow is laminar (25), although the high flow rates in some AVMs may produce turbulence in the venous drainage (25).

Although actual narrowing rates of AVM vessels following irradiation are not known,

representative values are chosen based on hemodynamic and flow alterations observed on follow-up cerebral angiographic examinations of our large series of patients with radiosurgically treated AVMs (7,8,9,16). Evaluation of two different rates of luminal narrowing demonstrates that there is no major difference in the temporal patterns of hemodynamic alterations post-radiosurgery; exponential decreases in AVM flow rate are observed in both cases. The only differences observed are that more rapid rates of luminal narrowing result in more rapid rates of AVM vessel closure and obliteration.

Calculations for complete-volume radiosurgical treatment of an AVM demonstrate an exponential decrease in blood flow until complete obliteration is achieved. However, there is a transient increase in blood pressure in the shunting arterioles. Mathematically, the hemodynamic resistance of the vessels in this compartment approaches infinity and the pressure gradient across the entire AVM exists in this single AVM compartment. Physiologically, hemostasis and vessel thrombosis are expected to occur once AVM blood flow has decreased to a certain critical level; blood flow through the AVM approaches zero and there is no longer any pressure gradient across the AVM. At this stage, the AVM is obliterated and the risk of hemorrhage is precluded.

These transient increases in pressure gradients are relatively small (4-8 mmHg), and may be within the range of physiological fluctuations in systemic blood pressure that occur in various normal activities such as exercise (12). This implies that the increased risk of hemorrhage from this transient rise in pressure may not be significant compared to the spontaneous rate of hemorrhage in untreated patients with cerebral AVMs. Therefore, although patients remain at risk for hemorrhage until the AVM is completely obliterated, there should be little or no increase in risk due to pressure changes following the radiosurgical procedure. We are presently examining the clinical results of our treatment series to assess this hypothesis.

In order to minimize the risks of radiation injury to normal brain surrounding an AVM, it is necessary to identify the core of the AVM and restrict stereotactic radiosurgery

in so far as possible to that target volume. It is still unclear how best to define the core of the AVM on cerebral angiography or CT and MRI scanning. From the point of view of blood flow dynamics, we define the AVM core as the hemodynamic or physiological center of the AVM through which all AVM blood flow must pass; it is not the anatomical center of the AVM shunts. In our compartmental flow model, the core of the AVM is comprised of the central core compartment (Fig 1a). For the partial-volume treatment approach is to be successful, all functional vessels in the core compartment must be irradiated. Our calculations demonstrate that, although the latency period for complete obliteration to occur is prolonged, AVM flow eventually decreases to zero if all aberrant vessels in the central core compartment are uniformly irradiated. However, there is a large increase in pressure in the core vessels which may increase the risk of hemorrhage before complete obliteration is achieved. This large rise in pressure in the core is only temporary (about 4-5 mon) and eventually all vessels in the core close off, blood flow through the AVM ceases, and pressure in this core compartment decreases to zero (Fig 5d). If all vessels in the core close off evenly and simultaneously, there should be no increased risk of hemorrhage from this rise in intraluminal pressure, as the thickened core vessel walls may be able to withstand this increase in pressure that arises naturally as a consequence of hemodynamic resistance increase and flow decrease. However, if some vessels in the central compartment close at a slower rate than others, resulting in differential flow and pressure dynamics in the different vascular shunts, then these vessels may be subjected to a very large increase in blood pressure which may, in turn, increase the risk of hemorrhage.

The above situation may exist in the partial-volume treatment of an AVM only if the radiosurgically-treated anatomical core corresponds with its true physiological core. If these do not correspond, then the untreated portion of the AVM may remain patent, resulting in persisting vascular shunts. In terms of the compartmental flow model, each AVM compartment is incompletely irradiated. Total AVM blood flow does not decrease to zero and permanent alterations in pressure profiles are obtained. The quantitative na-

ture of these alterations depends on the distribution of vessel radii and relative volume of each compartment treated. However, a persistent pressure increase in any compartment may result in an increased probability of hemorrhage from the residual shunts of the untreated AVM volume. We are presently testing the compartmental flow model in relation to dose-dependent, time-dependent, and volume-dependent variables involved in the vascular reaction of the AVM to radiation injury. These perturbations will be examined and applied to selected clinical observations in our patient series.

CONCLUSIONS

The complex and variable pathophysiology of intracranial AVMs makes it difficult to predict their precise temporal, morphologic, and pathophysiological response to radiosurgical treatment. AVMs vary considerably in size, shape, and location, but it is the abnormal hemodynamics of the AVM that cause the majority of its symptoms, particularly in high-volume, high-flow AVMs. A compartmental flow model has been developed based on current concepts of the functional anatomy of cerebral AVMs; such a model may prove to be a valuable method of analyzing the vascular and hemodynamic alterations that result following radiosurgery. With the introduction of multistage therapeutic strategies that include embolization, clipping of selected feeding vessels, and partial surgical resection, followed by radiosurgery, the altered hemodynamics become much more complex. It is necessary to understand the profound effects of these hemodynamic perturbations on the efficacy of the radiosurgical procedure. Our model is adaptable for varying latencies and obliteration rates depending on treatment volumes and radiation doses used, and these variables are presently being examined. The model can also be expanded to include analysis of steal and reperfusion phenomena by the addition of appropriate compartments to represent normal vasculature surrounding the AVM. Physiological adaptations may be examined by assuming nonlinear luminal narrowing rates. In this report, we have applied the model to analyze the differences between complete- and partial-volume radiosurgery of intracranial

AVMs. The initial results suggest that some permanent pressure and flow readjustments may occur as a result of partial-volume treatment strategies, and that this may lead to higher probabilities of hemorrhage from untreated shunts of the AVM.

Acknowledgments

We thank Dr. Alexander Nichols and Dr. Kerstin Rosander for many helpful discussions.

REFERENCES

1. Backlund EO, Arndt J, Dahlen H, Greitz T, Leksell L, Steiner L: Radiosurgery in intracranial arteriovenous malformations, in Carrea R (ed): *Neurological Surgery with Emphasis on Non-invasive Methods of Diagnosis and Treatment*, Amsterdam, Excerpta Medica, 1978, pp 162-167.

2. Batjer HH, Devous MD, Meyer YJ, Purdy PD, Samson DS: Cerebrovascular hemodynamics in arteriovenous malformation complicated by normal perfusion pressure breakthrough. Neurosurgery 22:503-509, 1988.

3. Batjer HH, Purdy PD, Giller CA, Samson DS: Evidence of redistribution of cerebral blood flow during treatment for an intracranial arteriovenous malformation. Neurosurgery 25:599-605, 1989.

4. Betti OO, Munari C, Rosler R: Stereotactic radiosurgery with the linear accelerator: treatment of AVMs. Neurosurgery 24:311-321, 1989.

5. Colombo F, Benedetti A, Casentini L: Narrow photon beam linear accelerator radiosurgery: six years experience. Proceedings of the International Workshop on Proton and Narrow Photon Beam Therapy, Oulu, Finland, pp 56-65, 1989.

6. Coulson JM, Richardson JF: Friction in pipes and channels, in *Chemical Engineering*, Oxford, Pergamon Press, 1977, pp 35-69.

7. Fabrikant JI, Lyman JT, Hosobuchi Y: Stereotactic heavy-ion Bragg peak radiosurgery for intracranial vascular disorders: method for treatment of deep arteriovenous malformations. Br J Radiol 57(678):479-490, 1984.

8. Fabrikant JI, Levy RP, Frankel KA, Phillips MH, Lyman JT, Chuang F, Steinberg GK, Marks MP: Sterotactic helium-ion radiosurgery for the treatment of intracranial arteriovenous malformations. Proceedings of the International Workshop on Proton and Narrow Photon Beam Therapy, Oulu, Finland, pp 33-37, 1989.

9. Fabrikant JI, Levy RP, Phillips MH, Lyman JT, Steinberg GK, DeLaPaz RL, Marks MP,

Chuang F: Clinical results of stereotatic heavy charged particle radiosurgery for intracranial arteriovenous malformations. Proceedings of Radiosurgery: a neurosurgical approach to intracranial lesions, University of Virginia, Charlottesville, 1989 (abstr).

10. Fabrikant JI: *Radiobiology*, Chicago, Year Book Medical, 1972.

11. Fung YC: *Biodynamics : Circulation*, New York, Springer-Verlag, 1984.

12. Guyton AC: *Texbook of Medical Physiology*, W.B.Saunders, 1981.

13. Khoroshkov VS, Goldin LL: Medical proton accelerator facility. Int J Radiat Oncol Biol Phys 15:973-978, 1988.

14. Kimmig B, Sturm V, Engenhart R, Wowra B, Marin-Grez M, Hover KH, van Kaick G: Stereotactic single high-dose radiation therapy of cerebral AVMs using a linear accelerator. Int J Radiat Oncol Biol Phys 15:226-230, 1988.

15. Kjellberg RN, Hanamura T, Davis KR, Lyons SL, Adams RD: Bragg peak proton-beam therapy for arteriovenous malformations of the brain. N Engl J Med 309:269-274, 1983.

16. Levy RP, Fabrikant JI, Frankel KA, Phillips MH, Lyman JT: Stereotactic heavy-charged particle Bragg peak radiosurgery for the treatment of intracranial arteriovenous malformations in childhood and adolescence. Neurosurgery 24:841-852, 1989.

17. Leussenhop AJ: Natural history of cerebral arteriovenous malformations, in Wilson CB, Stein BM (eds): *Intracranial Arteriovenous Malformations*, Baltimore/London, Williams and Wilkins, 1984, pp 12-23.

18. Lindegaard KF, Grolimund P, Aaaslid R, Nornes H: Evaluation of cerebral AVM's using transcranial Doppler ultrasound. J Neurosurg 65:335-344, 1986.

19. Lindqvist M, Steiner L, Blomgren H: Stereotactic radiation therapy of intracranial arteriovenous malformations. Acta Radiologica Suppl 369:610-613, 1986.

20. Lunsford LD, Flickinger J, Linndner G, Maitz A: Stereotactic radiosurgery of the brain using the first United States gamma knife. Neurosurgery 24:151-159, 1989.

21. McCormick WF: Pathology of vascular malformations of the brain, in Wilson CB, Stein BM (eds): *Intracranial Arteriovenous Malformations*, Baltimore/London, Williams

and Wilkins, 1984, pp 32-44.

22. Minakova YI, Krymsky VA, Luchin YI: Proton therapy on Synchrotron of the Institute for Theoretical and Experimental Physics in Moscow, a review of twenty years clinical experience. Proceedings of the International Workshop on Proton and Narrow Photon Beam Therapy, Oulu, Finland, p 18, 1989 (abstr).

23. Nornes H: Quantitation of altered hemodynamics, in Wilson CB, Stein BM (eds): *Intracranial Arteriovenous Malformations*, Baltimore/London, Williams and Wilkins, 1984, pp 32-43.

24. Nornes H, Grip A: Hemodynamic aspects of cerebral arteriovenous malformations. J Neurosurg 53:456-464, 1980.

25. Nornes H, Grip A, Wikeby P: Intraoperative evaluation of cerebral hemodynamics using directional Doppler technique Part 1: Arteriovenous Malformations. J Neurosurg 50:145-151, 1979.

26. Skalak R, Ozkaya N: Biofliud mechanics. Ann Rev Fluid Mech 21:167-204, 1989.

27. Spetzler RF, Selman WR: Pathophysiology of cerebral ischemia accompanying arteriovenous malformations, in Wilson CB, Stein BM (eds): *Intracranial Arteriovenous Malformations*, Baltimore/London, Williams and Wilkins, 1984, pp 12-23.

28. Steiner, L: Treatment of arteriovenous malformations by radiosurgery, in Wilson CB, Stein BM (eds): *Intracranial Arteriovenous Malformations*, Baltimore/London, Williams and Wilkins, 1984, pp 295-313.

29. Suhami L, Olivier A, Podgorsak EB, Pla M, Hazel J: Dynamic stereotactic radiosurgery: treatment results on 33 patients with AVM, Proceedings of the International Workshop on Proton and Narrow Photon Beam Therapy, Oulu, Finland, pp 72-76, 1989.

30. Yamada S: Arteriovenous malformations in the functional area: Surgical treatment and regional cerebral blood flow. Neurological Res 4(3/4):283-322, 1982.

31. Yamada S, Cojocaru T: Arteriovenous malformations, in Wood JH (ed): *Cerebral Blood Flow, Physiologic and Clinical Aspects*, New York, McGraw Hill, 1987, pp 580-592.

FIGURE LEGENDS

Figure 1a. The intracranial AVM is composed of a cluster of pathological vessels of varying sizes. The different vessel compartments serve as the basis for the compartmental flow model. (From Yamada S, Cojocaru T: Arteriovenous malformations, in Wood JH (ed): *Cerebral Blood Flow, Physiologic and Clinical Aspects*, New York, McGraw Hill, 1987, pp 580-592.) **b.** The intracranial AVM is modelled as a series of three linked flow compartments: the feeding arteries; the shunting arterioles; and the vessels of the central core. Blood flows from the cerebral arterial system into the AVM and drains into the cerebral venous system. Each flow compartment consists of parallel vessels of equal length with a Poisson distribution of vessel radii. The relative size of each compartment in this schematic diagram represents the blood volume in each flow compartment; it is greatest in the central core and least in the shunting arteriole compartment. The arrows represent the blood flow rates; flow rates are equal between compartments since they are linked serially.

Figure 2. AVM blood flow rate and pressure gradients in the different compartments following stereotactic radiosurgery. Vessel radii are decreased to simulate progressive narrowing of the AVM after radiosurgery. A variable initial induction period precedes the onset of radiation-induced hemodynamic alterations; plots demonstrate hemodynamic changes occuring after this initial induction period. Two different luminal narrowing rates are evaluated: (1) a radius-independent rate of 0.025 mm/mon (dotted lines); (2) a progressive radius-dependent rate where large vessels close off at 0.025 mm/mon until they reach a vessel radius of 0.2 mm, and thereafter close off at 0.05 mm/mon (solid lines). The plots are calculated for a *small* AVM according to parameters in **Table 1**. **a.** Blood flow rate through the AVM decreases exponentially from 150 ml/min to 0 ml/min as the AVM closes off completely. **b-d.** Alterations in pressure gradients across the three AVM compartments versus time are demonstrated.

Figure 3. Alterations in blood flow rate and pressure gradients in a *large* AVM, according to parameters in **Table 1**. **a.** Blood flow rate through the AVM decreases from 440 ml/min to 0 ml/min as the AVM closes off completely. **b-d.** Alterations in pressure gradients across the three AVM compartments versus time are demonstrated.

Figure 4. Lateral cerebral angiograms of a 38 year old male with a large left temporal lobe AVM. **a.** The large AVM demonstrates cerebral steal; normal perfusion to the surrounding vasculature is markedly reduced. The circumscribed area indicates the treatment target volume. **b.** One year after stereotactic radiosurgery (27 GyE, 230 MeV/u helium ions) the AVM is completely obliterated, and normal cerebral blood flow patterns are restored.

Figure 5. Alterations in blood flow rate and pressure gradients in a *large* AVM; the core compartment is completely irradiated but only 50% of vessels in the feeding arterial and shunting arteriole compartments are irradiated. **a.** The temporal pattern of blood flow rate through the partially-treated AVM is biphasic. There is an initial decrease in flow due to closure of smaller vessels in the shunting arteriole compartment, a brief plateau where minimal decrease in flow occurs for about 10 mon, followed by rapid decrease as the larger vessels in the completely-treated core are closed off. The time for complete obliteration is increased to 32-36 mon. **b-d.** The distribution of pressure gradients in the three AVM compartments with time differs markedly from that in the AVM that has received uniform irradiation to all compartments (cf **Fig 3**); the period of transient pressure increase in the shunting arterioles is prolonged and the core vessels of the central compartment are subjected to a large increase in blood pressure just before complete AVM obliteration. Note that the scale for the pressure axis in **d.** has been changed to accomodate the magnitude of the pressure increase in the core compartment (cf **Fig 2d, 3d, 6d**).

Figure 6. Alterations in blood flow rate and pressure gradients in a *large* AVM; only 50% of vessels in all three AVM compartments are irradiated. **a.** Blood flow rate does not decrease to zero as untreated vessels remain patent. **b-d.** Pressure gradients versus time across the

AVM compartments are altered permanently; blood pressure in the thin shunting arterioles is increased.

Figure 7. Lateral cerebral angiograms of a 20 year old male with a large right basal ganglia AVM. **a.** The circumscribed area indicates the treatment target volume, which included only the anterior portion of the AVM. **b.** One year after stereotactic radiosurgery (20 GyE, 230 MeV/u helium ions), the treated volume has undergone obliteration, with concommitant reduction in size of its feeding artery. However, the posterior portion of the AVM remains patent, and the feeding vessel has increased in size, resulting in an increased rate of blood flow through the untreated AVM shunts.

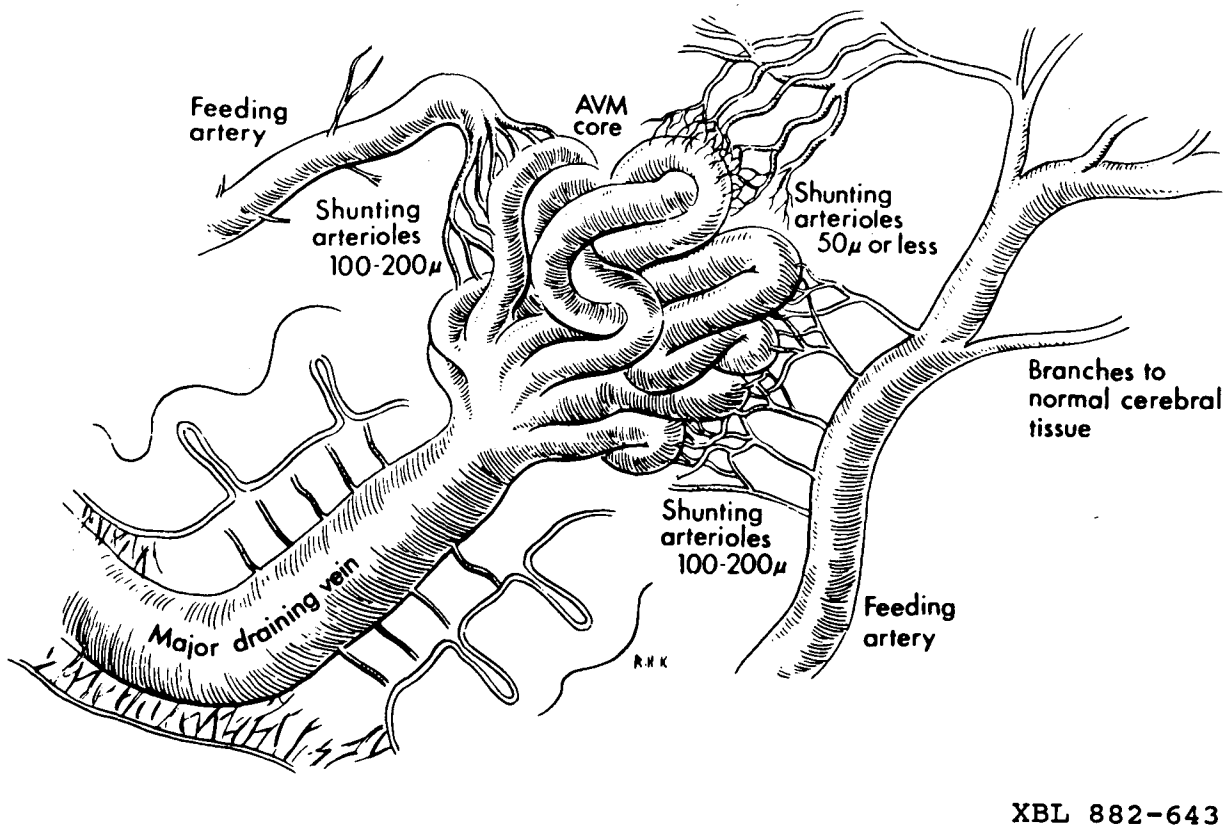

Figure 1A

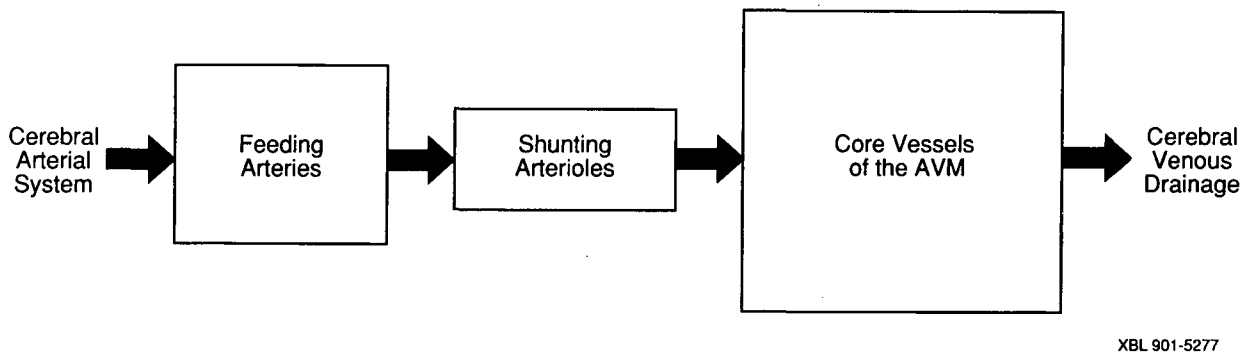

Figure 1B

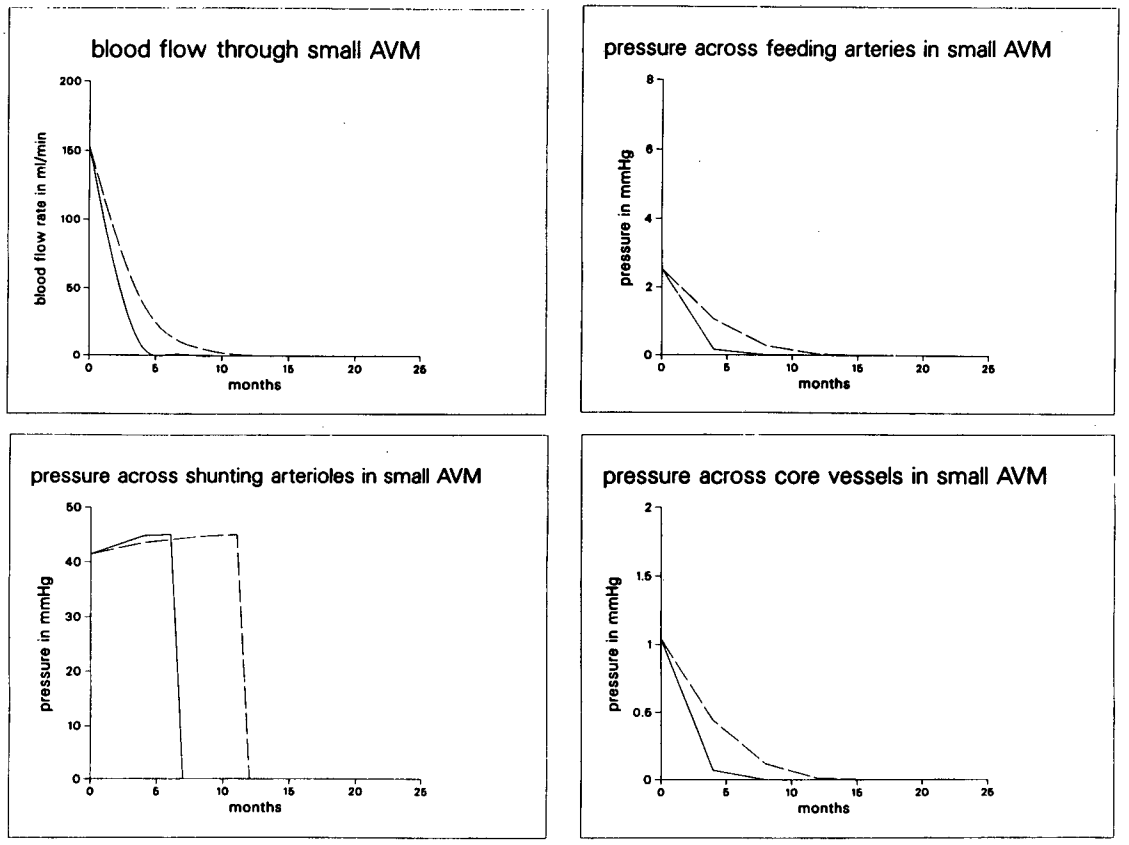

XBL 901-156

Figure 2A-D

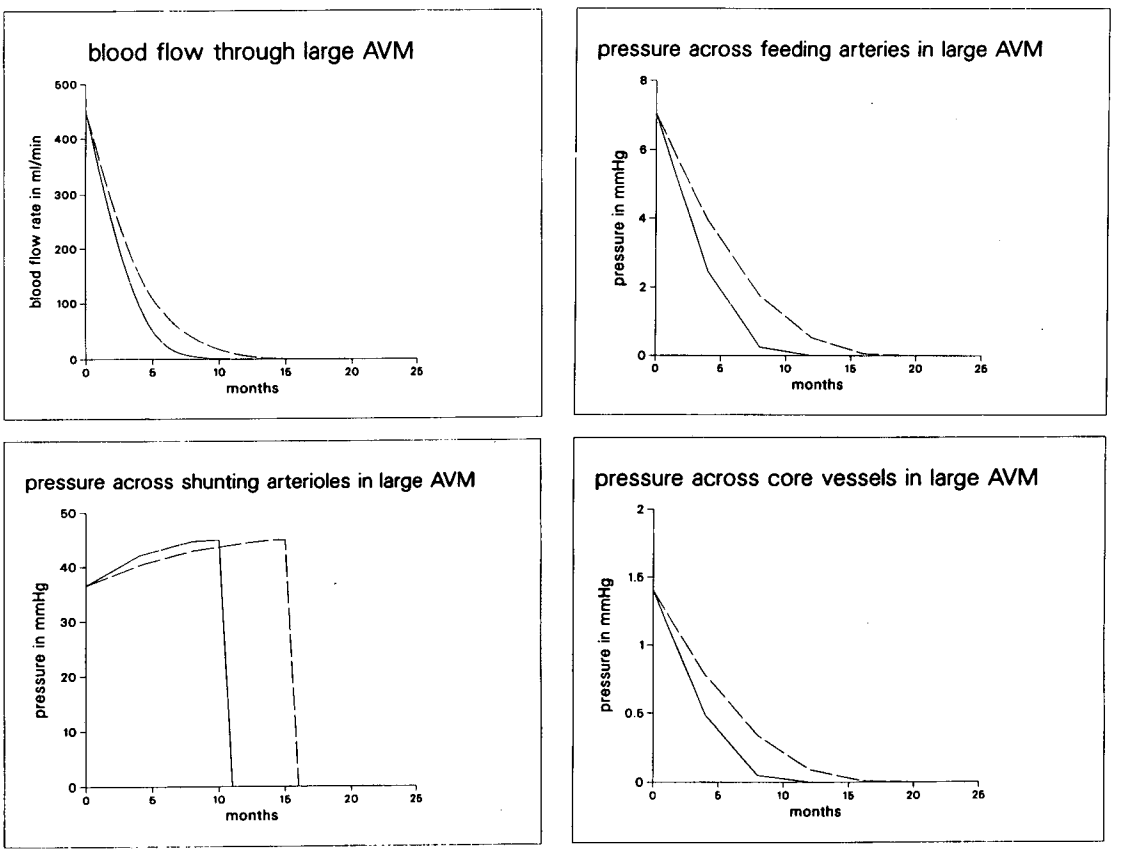

Figure 3A-D

XBL 901-154

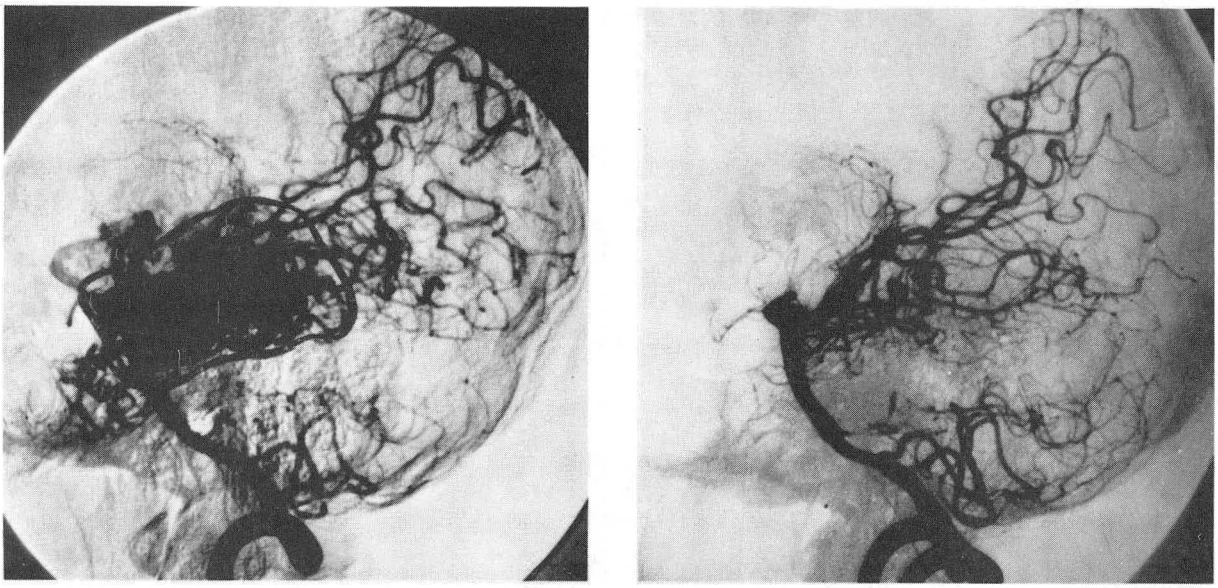

XBB 876-5281B

Figure 4A-B

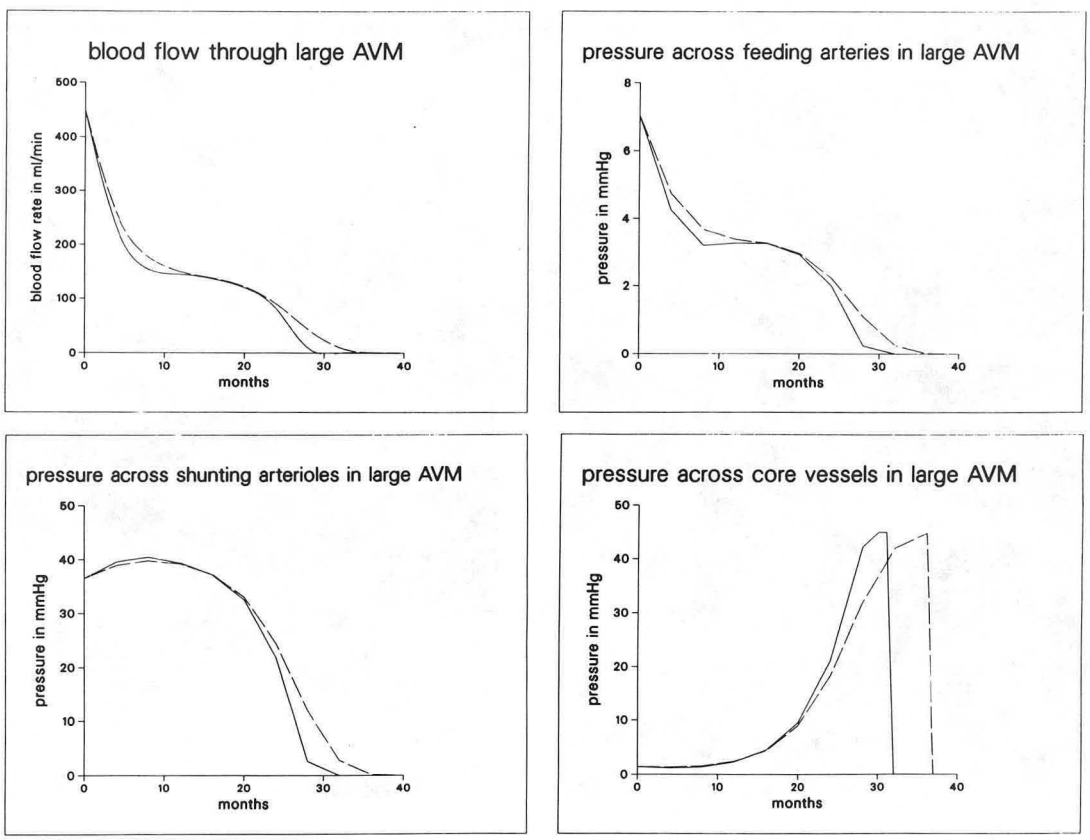

XBL 901-155

Figure 5A-D

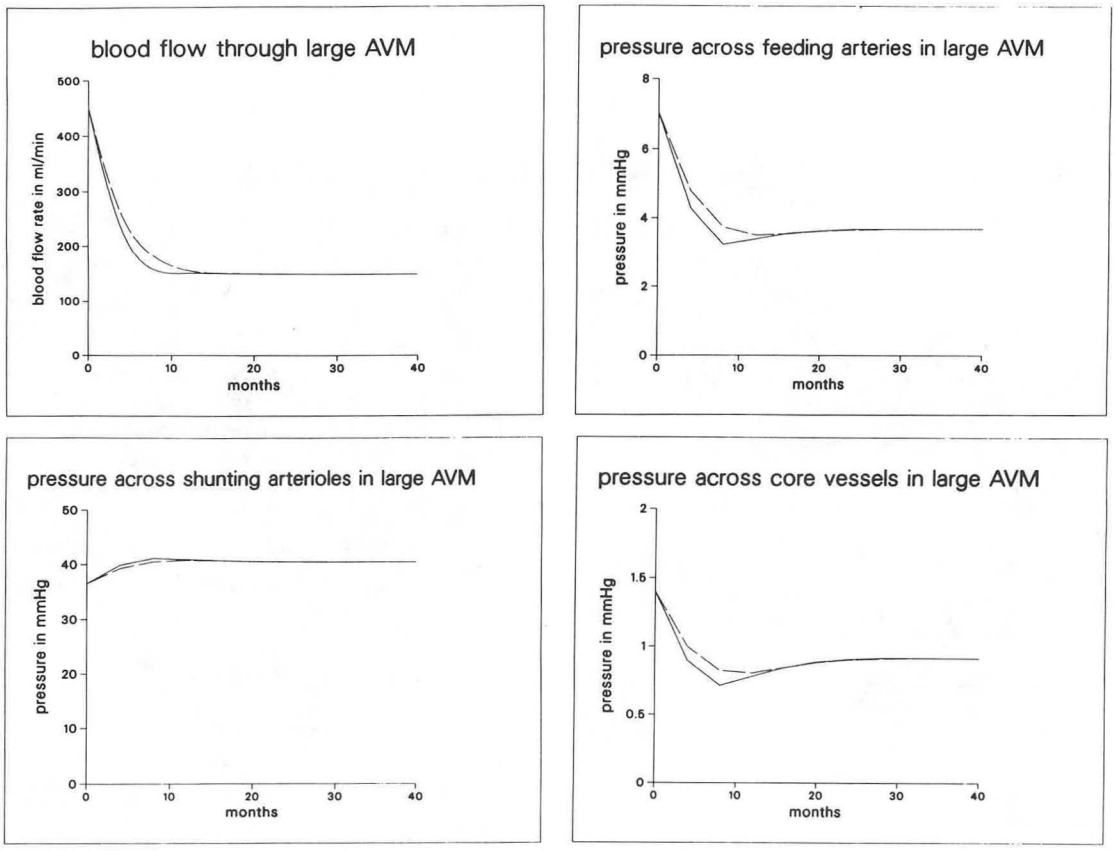

Figure 6A-D

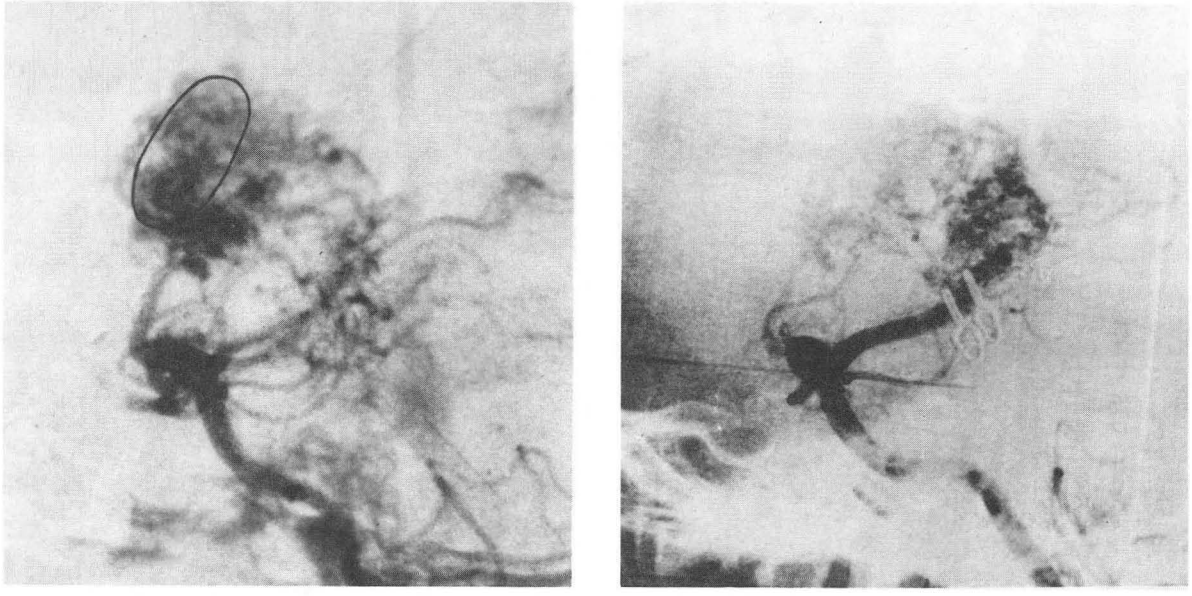

XBB 890-8866A

Figure 7A-B

TABLE 1

INITIAL PARAMETERS FOR COMPARTMENTAL FLOW MODEL OF INTRACRANIAL ARTERIOVENOUS MALFORMATIONS

	Small AVM			*Large* AVM		
Compartments	Feeding Arteries	Shunting Arterioles	Core Vessels	Feeding Arteries	Shunting Arterioles	Core Vessels
Number of vessels in each compt. (N)	4	10	20	5	20	40
Length of vessels in each compt. (l)	3.0 cm	1.0 cm	5.0 cm	3.0 cm	1.0 cm	5.0 cm
Average vessel radius (r)	0.1 cm	0.01 cm	0.1 cm	0.1 cm	0.01 cm	0.1 cm
Pressure gradient (ΔP)	2.5 mmHg	41.4 mmHg	1.1 mmHg	7 mmHg	36.5 mmHg	1.5 mmHg
Total AVM blood flow	150 ml/min			440 ml/min		

LAWRENCE BERKELEY LABORATORY
TECHNICAL INFORMATION DEPARTMENT
1 CYCLOTRON ROAD
BERKELEY, CALIFORNIA 94720